

The Development of an Active Roll Control System for Heavy Vehicles

D.J.M. SAMPSON, G. McKEVITT AND D. CEBON*

SUMMARY

This paper describes the development of an active roll control system for a tractor semi-trailer. The design of the roll control system hardware and software are detailed. Simulations of the yaw-roll response of the vehicle show that the system will provide significant improvements in rollover stability.

1. INTRODUCTION

1.1. Background

Studies have shown that most rollover accidents involve heavy articulated vehicles, and occur on highways [1]. Three major contributing factors to rollover accidents have been identified: (1) sudden course deviation, often in combination with heavy braking, from high initial speed; (2) excessive speed on curves; and, (3) load shift. The accidents are relatively frequent, and the estimated average cost to operators is between USD 120,000 and 160,000 [2].

1.2. Previous Research

Although research into the use of active suspension systems on automobiles has been extensive, the use of active suspension systems on heavy articulated vehicles, particularly to control roll motion, has been researched to a relatively small degree [1,3]. However, several researchers have indicated potential improvements in rollover safety are possible, even when using relatively low-power, low-bandwidth actuators to control the active suspension system.

Dunwoody [4] simulated the steady state cornering performance of a tractor semi-trailer fitted with an active roll control system. The system consisted of a hydraulically tiltable fifth wheel coupling and hydraulic actuators that could apply control torques to each of the trailer axles. The control system measured the trailer lateral acceleration and the relative roll angle between the tractor and the trailer, and the study found such a system could raise the static rollover threshold by 20-30%.

Lin et al. [5,6] investigated the use of active roll control on a single unit truck using a simple linear model. The performances of systems based on roll angle feedback, lateral acceleration feedback and load transfer feedback were investigated. Control gains were selected by pole placement. The authors recommended using a

* Cambridge University Engineering Department, Trumpington Street, Cambridge CB2 1PZ. U.K.

control system based on lateral acceleration feedback, which demonstrated several key benefits: (1) the ability to tilt vehicle into a corner, providing significant improvements in load transfer; (2) fast transient response; and, (3) relatively simple instrumentation requirements. The study reported that such a system could provide worthwhile reductions in transient and steady state load transfer of up to 30%. Lin et al. [5,6] also investigated the performance of a roll control system designed using an optimal state feedback technique and a steering input power spectrum based on road alignment data and pseudo-random lane changes. The system performance was marginally superior to that of the lateral acceleration feedback controller.

Lin et al. [5,7] simulated the performance of a tractor semi-trailer with torsionally rigid frames, fitted with a roll control system. The controller was based on lateral acceleration feedback. Control gains were selected by pole placement. The study found that such a system could reduce steady state and transient load transfer for a range of manoeuvres. The study recommended investigating the influence of vehicle frame flexibility on control system performance.

Sampson and Cebon [8] proposed a vehicle roll control system design methodology based on a linear quadratic regulator. The study found that this design technique allowed the control system designer to make trade-offs between performance and power consumption requirements when designing multiple-actuator roll control systems for tractor semi-trailers and long combination vehicles.

1.3. CVDC Experimental Vehicle

The roll control system described in this paper is one sub-system of a computer-controlled experimental vehicle being developed by the Cambridge Vehicle Dynamics Consortium (CVDC). The system consists of five active anti-roll bars (two on the tractor and three on the semi-trailer) driven by ten hydraulic actuators under computer control. The air suspension systems on the vehicle also incorporate a ride control system consisting of ten high-performance continuously variable semi-active dampers, which are being developed by Koni BV [9]. A yaw control system, implemented by enhancing the algorithms of the vehicle's electronic braking system, is currently at an early stage of development. In their final forms, the three systems will work together to provide integrated control of the vehicle's ride, yaw and roll motions.

Design and development of the anti-roll hardware is a significant challenge, given the large forces, torques and roll-rates needed for effective control. This paper will address the key practical constraints, including component strengths and hydraulic limits (power, flow and pressure). The design and development of the control system software is also governed by challenging performance and safety requirements.

2. VEHICLE MODELLING

2.1. Modelling approach

The vehicle model used in the design and analysis of the roll control system is intended to capture the essential handling and roll dynamics. Other vehicle motions, such as bounce and pitch, are of secondary importance.

The model is an extension of the simple three degree of freedom single unit yaw-roll model developed by Segel [10]. The tractor and semi-trailer are each modelled

with one vehicle unit, and the two units are hitched together with a fifth wheel coupling. The sprung and unsprung masses of both the tractor and trailer unit are represented by lumped masses, with each vehicle unit having yaw, sideslip, front roll and rear roll freedoms (Fig. 1). The front and rear sections are coupled with a torsionally-flexible frame. The axles of each vehicle unit are considered to be rigid bodies, with flexible tyres that can roll with respect to the suspension roll axis. The sprung masses roll about the roll axis, and are restrained by the roll stiffness and damping of the suspension. Control torques u_f and u_r , representing the torques applied by the active roll control system, act on each section of the sprung mass.

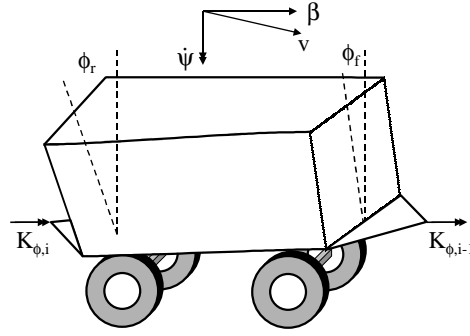


Fig. 1. Schematic diagram of a generic vehicle unit.

2.2. Equations of motion

Each vehicle unit has six equations of motion. Notation is listed in the Appendix.

Lateral force equation:

$$m_{s,f,i} h_{f,i} \ddot{\phi}_{f,i} + m_{s,r,i} h_{r,i} \ddot{\phi}_{r,i} + m_i v (\dot{\beta}_i + \dot{\psi}_i) = Y_{\beta,i} \beta_i + Y_{r,i} \dot{\psi}_i + Y_{\delta,i} \delta_i + F_{i-1} - F_i \quad (1)$$

Yaw moment equation:

$$-I_{xz,f,i} \ddot{\phi}_{f,i} - I_{xz,r,i} \ddot{\phi}_{r,i} + I_{z,i} \ddot{\psi}_i = N_{\beta,i} \beta_i + N_{r,i} \dot{\psi}_i + N_{\delta,i} \delta_i + x_{f,i} F_{i-1} - x_{r,i} F_i + K_{\psi,i-1} (\psi_{i-1} - \psi_i) - K_{\psi,i} (\psi_i - \psi_{i+1}) \quad (2)$$

Front sprung mass roll moment equation:

$$I_{x,f,i} \ddot{\phi}_{f,i} + m_{s,f,i} h_{f,i} (\dot{\beta}_i + \dot{\psi}_i) - I_{xz,f,i} \ddot{\psi}_i = m_{s,f,i} g h_{f,i} \phi_{f,i} - K_{f,i} (\phi_{f,i} - \phi_{t,f,i}) - L_{f,i} (\dot{\phi}_{f,i} - \dot{\phi}_{t,f,i}) + u_{f,i} - K_{c,i} (\phi_{f,i} - \phi_{r,i}) - L_{c,i} (\dot{\phi}_{f,i} - \dot{\phi}_{r,i}) - F_c h_c + K_{\phi,i-1} (\phi_{r,i-1} - \phi_{f,i}) - z_{f,i} F_{i-1} \quad (3)$$

Rear sprung mass roll moment equation:

$$\begin{aligned}
I_{x,r,i}\ddot{\phi}_{r,i} + m_{s,r,i}h_{r,i}(\dot{\beta}_i + \dot{\psi}_i) - I_{xz,r,i}\ddot{\psi}_i = \\
m_{s,r,i}gh_{r,i}\phi_{r,i} - K_{r,i}(\phi_{r,i} - \phi_{t,r,i}) - L_{r,i}(\dot{\phi}_{r,i} - \dot{\phi}_{t,r,i}) + u_{r,i} \\
+ K_{c,i}(\phi_{f,i} - \phi_{r,i}) + L_{c,i}(\dot{\phi}_{f,i} - \dot{\phi}_{r,i}) + F_c h_c \\
- K_{\phi,i}(\phi_{r,i} - \phi_{f,i+1}) - z_{r,i}F_i
\end{aligned} \quad (4)$$

where F_c is the shear force in the vehicle chassis:

$$\begin{aligned}
F_c = F_{i-1} + (Y_{\beta,f,i}\beta_{f,i} + Y_{r,f,i}\dot{\psi}_i + Y_{\delta,f,i}\delta_{f,i}) \\
- (m_{s,f,i} + m_{u,f,i})v(\dot{\beta}_i + \dot{\psi}_i) - m_{s,f,i}h_{f,i}\ddot{\phi}_{f,i}
\end{aligned}$$

Front unsprung mass roll moment equation:

$$\begin{aligned}
r(Y_{\beta,f,i}\beta_{f,i} + Y_{r,f,i}\dot{\psi}_i + Y_{\delta,f,i}\delta_{f,i}) + m_{u,f,i}h_{u,f,i}v(\dot{\beta}_i + \dot{\psi}_i) = \\
K_{t,f,i}\phi_{t,f,i} - K_{f,i}(\phi_{f,i} - \phi_{t,f,i}) - L_{f,i}(\dot{\phi}_{f,i} - \dot{\phi}_{t,f,i}) + u_{f,i}
\end{aligned} \quad (5)$$

Rear unsprung mass roll moment equation:

$$\begin{aligned}
r(Y_{\beta,r,i}\beta_{r,i} + Y_{r,r,i}\dot{\psi}_i + Y_{\delta,r,i}\delta_{r,i}) + m_{u,r,i}h_{u,r,i}v(\dot{\beta}_i + \dot{\psi}_i) = \\
K_{t,r,i}\phi_{t,r,i} - K_{r,i}(\phi_{r,i} - \phi_{t,r,i}) - L_{r,i}(\dot{\phi}_{r,i} - \dot{\phi}_{t,r,i}) + u_{r,i}
\end{aligned} \quad (6)$$

The motions of the tractor and trailer units are coupled by a kinematic constraint equation at the fifth wheel.

$$\beta_i - \beta_{i+1} - \frac{z_{r,i}}{v}\dot{\phi}_{r,i} + \frac{z_{f,i}}{v}\dot{\phi}_{f,i} + \frac{x_{r,i}}{v}\dot{\psi}_{r,i} - \frac{x_{f,i}}{v}\dot{\psi}_{f,i} + \psi_i - \psi_{i-1} = 0 \quad (7)$$

The equations of motion of the combined vehicle are formulated into a state space representation, and the response of the vehicle to steady cornering and transient manoeuvres such as lane changes can be simulated. The same general model formulation can be used with any number of generic vehicle units, coupled together with a variety of hitch mechanisms, to model long combination vehicles.

A simple tyre model represents the change in tyre cornering stiffness with vertical load. Limitations in the available torque and the response time of the hydraulic actuators are also included.

3. SUSPENSION HARDWARE

3.1. Conceptual design

The trailer suspension is a modified *Indair* air suspension unit from Meritor HVS, which consists of two independent trailing arms hinged from a transverse beam.

The active roll control system consists of a stiff U-shaped anti-roll bar, connected at each end to the trailing arms, and two hydraulic actuators located between the

chassis and anti-roll bar (Fig. 2). The actuators apply equal and opposite vertical loads to the bar, thereby twisting it, and applying a roll moment to the vehicle body. The result is a floating anti-roll bar whose position is determined by the wheel positions and the actuator positions. Use of a single hydraulic actuator would have been considerably simpler, but was not possible because the much larger stroke requirement exceeded the available space under the vehicle.

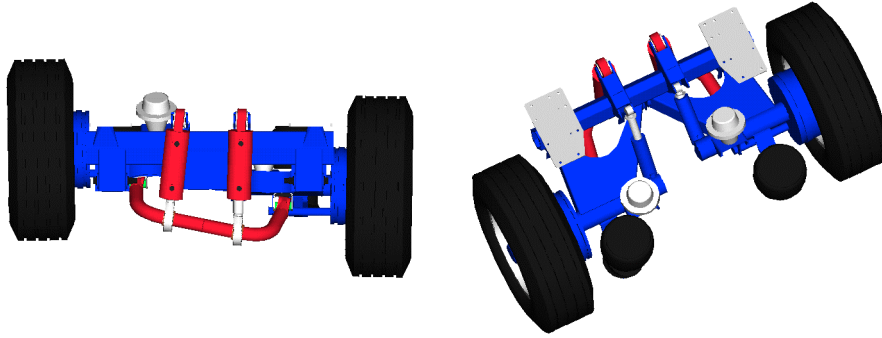


Fig. 2. Solid model of the modified trailer suspension, showing the location of the actuators and the anti-roll bar: (a) elevation looking towards the rear; (b) perspective view from above, looking forwards.

3.2. Actuator specifications

An analysis of the kinematics and dynamics of the roll control system was performed to determine the required stroke and size of the hydraulic actuators.

The stroke required to move the sprung mass to the maximum roll angle (as limited by the suspension travel) of $\pm 6.1^\circ$ was 85 mm.

The maximum required actuator force was determined for both steady state and transient manoeuvres.

The maximum steady state force is that required to hold the sprung mass at zero roll angle during in 0.5 g steady state turn. (The rollover threshold of the vehicle is 0.5 g.) This force was calculated to be 110 kN.

The worst case transient force is that required to drive the sprung mass sinusoidally at a given frequency with the maximum amplitude of roll angle. Fig. 3(a) shows the forces acting on the tanker body in the dynamic case. There are forces from the springs (F_{spring}), the dampers (F_{damper}), the actuators (F_{ARB}), and the bushes at the trailing arm mounting points (R_1 and R_2). Fig. 3(b) shows the forces on the trailing arm.

The reaction forces at the bushes are given by:

$$R_1 = \frac{\gamma_1 F_{ARB} + \gamma_2 F_{spring} + \gamma_3 F_{damper}}{x_{TA}} \quad (8)$$

$$R_2 = -\gamma_4 F_{spring} - \gamma_5 F_{damper} - \gamma_6 F_{ARB} \quad (9)$$

where $\gamma_1, \dots, \gamma_6$ are functions of the suspension geometry [11].

Taking the sum of moments about the trailer roll centre gives an expression for the dynamic actuator force:

$$F_{ARB} = \frac{I_{xx}\ddot{\phi} + \eta_3 c_{damper} d_{damper} \dot{\phi} + \left[\eta_2 k_{spring} \left(\frac{l_{spring} d_{damper}}{l_{damper}} \right) - m_s g h \right] \phi}{\eta_1} \quad (10)$$

where η_1, \dots, η_3 are also functions of the suspension geometry [11].

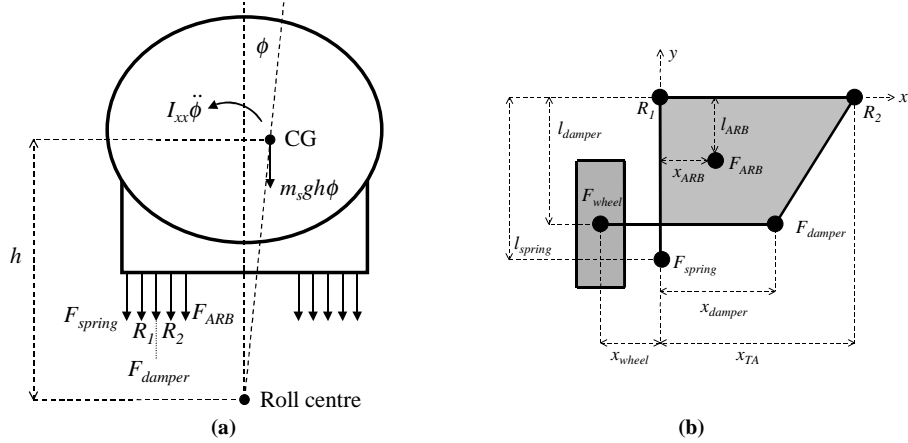


Fig. 3. Free body diagrams used to determine the dynamic actuator force requirements: (a) elevation view of the tanker; (b) plan view of the trailing arm (the y-axis is parallel to the longitudinal axis of the vehicle).

The dependence of actuator force requirement on actuation frequency is shown in Fig. 4. The system has a roll resonance at 1.8 Hz. This places an upper limit on the achievable system bandwidth of approximately 1.2 Hz. The maximum actuator force requirement below this frequency is the DC value of 128 kN. The actuators selected to meet this specification have 125 mm bore, and produce 137 kN for a rod diameter of 56 mm and a pressure of 210 bar. The large actuator force necessitates a large piston area, and thus large fluid flows through the actuator. For a 1 Hz oscillation, a cylinder of volume 1.1 L requires a flow rate of $2.2 \text{ L}\cdot\text{s}^{-1}$. The limited flow rate through the servo-valves of a mobile hydraulic system further constrains the achievable response bandwidth of the roll control system. Accumulators are used to store hydraulic fluid to allow the system to operate for a limited number of extend-retract cycles, but continuous harmonic motion is not possible indefinitely.

The possibility of cross-linking the two air springs at either end of each axle, with a large diameter pipe, was investigated. Such a system greatly reduces the force requirement at low frequencies by effectively eliminating the roll stiffness of the suspension. The actuator force requirement as a function of frequency for the cross-linked system is also shown in Fig. 4. Cross-linking the air springs eliminates the roll resonance at 1.8 Hz, but the required actuator force rises sharply with actuation frequency. The achievable system bandwidth is limited by the maximum actuator force, rather than by resonance in the roll motion. For example, a maximum actuator force of 128 kN gives a system bandwidth of 1.7 Hz, which is an improvement over the 1.2 Hz for the independent air spring configuration.

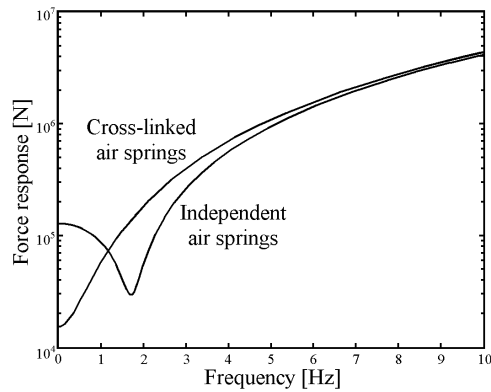


Fig. 4. Dynamic actuator force required for harmonic roll excitation of the sprung mass.

However, the improved performance of the cross-linked system has a key safety drawback: the vehicle is unstable in roll in the event of a failure in the active control system. Complex safety features such as emergency lock-off valves and monitoring systems would need to be fitted to ensure the fail safety of the system. Thus, the system based on independent air springs was selected for implementation on the initial prototype vehicle.

3.3. Other modifications

The transverse hexagonal beam on the Indair suspension was extensively reinforced so that it could carry the large additional loads transmitted through the hydraulic actuators.

4. CONTROLLER DESIGN AND IMPLEMENTATION

4.1. Architecture

A distributed controller architecture, consisting of a central control unit and multiple local control units, has been adopted. The distributed architecture was selected to simplify the physical installation, maximise real-time performance, and enable modular code development and rapid prototyping.

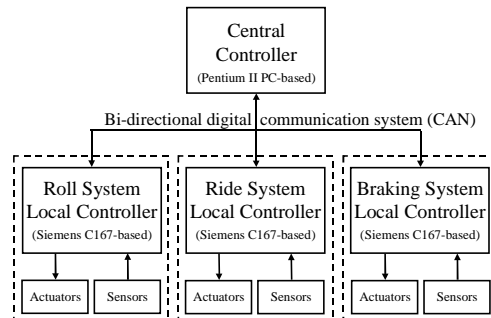


Fig. 5. Distributed controller architecture for the experimental vehicle.

The central control unit executes the *high level* vehicle dynamics control code, as well as providing safety monitoring. The *low level* local control units control individual actuators and acquire sensor data. The central and local control units are linked together by a CAN bus, over which the central controller sends demand signals to the local controllers, and the local controllers send sensor data to the central controller.

4.2. Local controller design

The local controllers control the motion of the hydraulic actuators in response to demand signals from the global controller. Fig. 6 shows that the local controller comprises a roll moment controller and an actuator controller [11]. The roll moment controller (a PID controller with a lag pre-filter) is the main component of the local controller. However, because a floating anti-roll bar arrangement is used, the local controller also includes an actuator controller that ensures that the centre of the anti-roll bar is held at the neutral displacement (i.e. the centre of the actuator stroke). The actuator controller is necessary to ensure sufficient ground clearance and to enable maximum roll stroke to be achieved. The dynamics of the vehicle system and the feedback sensors complete the feedback loop. The actuator model captures several limitations in the control system hardware, notably the limits on maximum actuator force, maximum flow rate through the servo-valve, and bandwidth of the servo-valve. The flexibilities of the mechanical and hydraulic components in the active anti-roll bar assembly are included in the vehicle and actuator models.

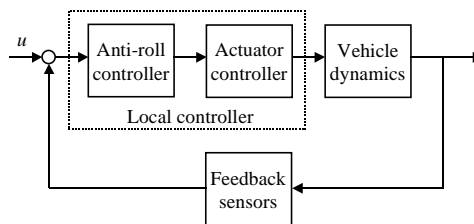


Fig. 6. Block diagram of the local controller system.

Gains for the local controller were selected using pole placement, with the aims of ensuring robust stability and good steady state tracking of the demand torques, and well as a fast rise time, fast settling time and smooth step response. The local control system has a rise time of approximately 0.3 s in response to a large step-shaped roll torque demand signal of 60 kN.m [11]. This is sufficiently fast for this application, especially given that the steering input spectrum that forces the vehicle roll motion is concentrated below 1 Hz [5].

4.3. Global controller design

The global roll controller processes signals from instrumentation on the vehicle, and sends demand signals for roll torques to the local controllers at each axle.

The objective of the roll control system is to minimise lateral load transfer in response to steering inputs, since it is excessive lateral load transfer that causes vehicle rollover. Lateral load transfers due to centripetal acceleration and lateral coupling forces are set by the vehicle dimensions and trajectory. However, other load transfer terms, due to vehicle body roll and torques applied by adjacent vehicle

units through couplings, are strongly influenced by the performance of the suspension and the active roll control system.

The roll control system is designed to work using simple instrumentation. The lateral acceleration at the centres of mass of the tractor and trailer is measured, as are the roll rates of both vehicle units.

The gains for the global controller were selected using pole placement. The proportional gains on the lateral acceleration signals were designed to give equal rollover thresholds at each axle during steady state cornering, thereby maximising the rollover threshold of the vehicle as a whole. High gains on lateral acceleration, which are necessary to tilt the vehicle units into the turns, caused instabilities in the roll dynamics. However, these instabilities were stabilised by adding roll rate feedback, which increases the damping of the roll modes. The root locus plot in Fig. 7 shows the effects of lateral acceleration and roll rate feedback on the stability and speed of trailer axle feedback loop. Attempts to stabilise the system using derivative feedback on lateral acceleration proved ineffective.

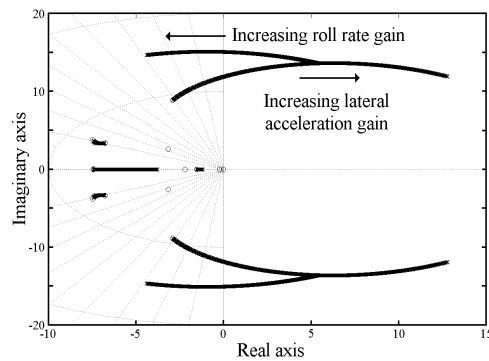


Fig. 7. Root locus plot for trailer axle roll control feedback loop, showing the effects of lateral acceleration gain and roll rate gain on system stability.

The performance of the active roll control system is compared with that of a passive suspension system for a severe lane change manoeuvre in Figs. 8 and 9. The rollover threshold of the active vehicle is increased because the control system is able to tilt the vehicle into turns, reducing load transfer. The normalised load transfer of both the tractor and trailer units are reduced by around 25% over the passive system. The roll angle into the turn of the tractor is greater than that of the trailer. This difference in roll angles produces a torque between the tractor and trailer that is transmitted through the stiff fifth wheel coupling. This torque further reduces the load transfer at the trailer axles. The benefits that can be obtained using this *roll moment co-operation* effect are limited if the fifth wheel or the trailer chassis is very flexible in roll.

Simulations of the response of the active system during steady cornering indicate that reductions in load transfer of around 20% are possible.

The roll torque is distributed among the axles, rather than concentrated at any one axle. This strategy avoids excessively high reductions in cornering performance at any one axle, and minimises the degradation in vehicle handling performance.

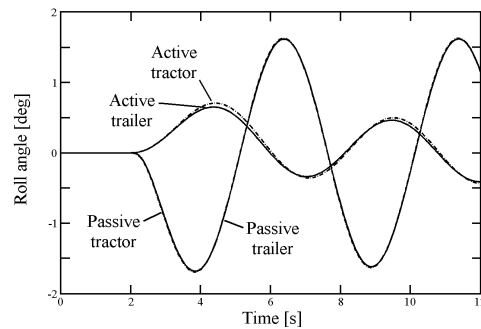


Fig. 8. Roll angle response of active and passive vehicles during a lane change manoeuvre.

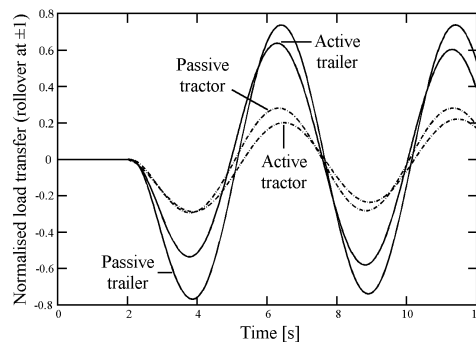


Fig. 9. Load transfer response of active and passive vehicles during a lane change manoeuvre.

4.4. Hardware

The central controller has been implemented on an Intel Pentium II 400 MHz PC. The control code runs under a real-time kernel by RealTech AG. The central control system software is developed in MATLAB and Simulink, compiled to C code, and then downloaded to the central controller PC.

The local controllers have been implemented using Siemens C167 microprocessors. The C167 features on-board A/D and D/A conversion and an on-board CAN interface, as well as numerous digital I/O lines. Components for signal conditioning and memory are also mounted on the local controller printed circuit boards. The local control system software is developed in C and downloaded to the microprocessors.

5. CONCLUSIONS

An active roll control system, based on a modified passive suspension system, has been developed for a tractor semi-trailer. The system uses active anti-roll bars, controlled by hydraulic actuators, to control roll motion at each axle.

The active roll control system uses a distributed controller architecture. Microprocessor-based local controllers control the individual actuators, while a PC-based global controller monitors vehicle dynamics and safety functions. The global

and local controllers communicate over a CAN bus. The distributed architecture simplifies installation, optimises performance and allows rapid prototyping.

Simulations of the yaw-roll performance of a tractor semi-trailer fitted with the active roll control system indicate that system will provide steady state and transient improvements of up to 25% of the rollover stability of the vehicle. The system uses simple instrumentation to measure the lateral acceleration and roll rate of the tractor and trailer. Further development of the control strategies is ongoing.

A prototype vehicle fitted with the active roll control system will be tested shortly.

ACKNOWLEDGEMENTS

The authors wish to acknowledge the financial support of the Cambridge Vehicle Dynamics Consortium and the Engineering and Physical Sciences Research Council. The Cambridge Vehicle Dynamics Consortium consists of the Universities of Cambridge, Cranfield and Nottingham together with the following industrial partners from the European heavy vehicle industry: Tinsley Bridge Ltd, Meritor HVS, Koni BV, DERA, Dunlop Tyres, Shell UK Ltd, Volvo Trucks and Crane Fruehauf. The authors also wish to thank Ben Jeppesen and Richard Roebuck for their help and advice with various aspects of the project. Mr Sampson would like to thank the Cambridge Australia Trust and the Committee of Vice-Chancellors and Principals of the Universities of the United Kingdom for their support.

REFERENCES

1. Kusters, L.J.J.: Increasing roll-over safety of commercial vehicles by application of electronic systems. *Smart Vehicles*. Pauwelussen J.P. and Pacejka H.B. ed., Swets and Zeitlinger, 1995, pp. 362-377.
2. Harris, R.: Cost of roll-over accidents. Personal communication, 1995.
3. Besinger, F.H., Cebon, D. and Cole, D.J.: Force control of a semi-active damper. *VSD*, Vol. 24 (No. 1), 1995, pp. 695-723.
4. Dunwoody, A.B.: Active roll control of a semi-trailer. *SAE Transactions*, SAE 933045 (Nov), 1993.
5. Lin, R.C.: An investigation of active roll control for heavy vehicle suspensions. PhD thesis, Cambridge University Engineering Department, 1994.
6. Lin, R.C., Cebon, D. and Cole, D.J.: Optimal roll-control of a single-unit lorry. *J. Auto. Eng., Proc. IMechE*, D05294, 1996, pp. 45-55.
7. Lin, R.C., Cebon, D. and Cole, D.J.: Active roll control of articulated vehicles. *VSD*, Vol. 26 (No. 1), 1996, pp. 17-43.
8. Sampson, D.J.M. and Cebon, D.: An Investigation of Roll Control System Design for Articulated Heavy Vehicles. *Proc. AVEC '98*, Nagoya, Japan, 1998, pp 311-316.
9. De Koch, C.: Development of a new continuously variable damper for semi-active suspensions. *IMechE publication C389/471*, 1992, pp 141-151.
10. Segel, L.: Theoretical prediction and experimental substantiation of the response of an automobile to steering control. *Proc. IMechE Automobile Division*, 1956-1957, pp. 310-330.
11. McKeivitt, G.: Design of roll control systems for heavy vehicles. MPhil thesis, Cambridge University Engineering Department, 1999.

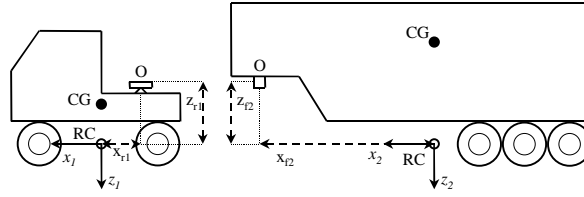
APPENDIX: NOTATION

ψ	Heading angle	m_s	Sprung mass
$\dot{\psi}$	Yaw rate	m_u	Unsprung mass

ϕ	Sprung mass roll angle	I_x	Roll moment of inertia
ϕ_t	Unsprung mass roll angle	I_z	Yaw moment of inertia
β	Sideslip angle	I_{xz}	Product of inertia
δ	Steering angle	F	Lateral force in coupling
v	Vehicle speed	K_ϕ	Coupling roll stiffness
u	Active roll torque	F_c	Shear force in vehicle frame
K	Suspension roll stiffness	h_c	Vehicle frame centroid height
L	Suspension roll damping	K_c	Frame roll stiffness
K_t	Tyre roll stiffness	h	Sprung mass height
r	Roll centre height	h_u	Unsprung mass height

The subscript i denotes vehicle unit i or coupling i . Coupling i is the coupling between vehicle units i and $i+1$. The subscript j denotes axle j . The subscript f denotes the front section of a vehicle unit, while the subscript r denotes the rear section of the vehicle unit. Vehicle units, couplings and axles are numbered from front to rear.

Other dimensions are as shown:



The tyre coefficients in Eqs. 1-6 are given by:

$$Y_{\beta,i} = \frac{\partial F_i}{\partial \beta_i} = \sum_j c_{i,j}$$

$$N_{\beta,i} = \frac{\partial M_i}{\partial \beta_i} = \sum_j a_j c_{i,j}$$

$$Y_{r,i} = \frac{\partial F_i}{\partial \psi_i} = \sum_j \frac{a_j c_{i,j}}{v}$$

$$N_{r,i} = \frac{\partial M_i}{\partial \psi_i} = \sum_j \frac{a_j^2 c_{i,j}}{v}$$

$$Y_{\delta,i} = \frac{\partial F_i}{\partial \delta_i} = -\sum_j c_{i,j}$$

$$N_{\delta,i} = \frac{\partial M_i}{\partial \delta_i} = -\sum_j a_j c_{i,j}$$

where a is the distance from the centre of mass to the axle and c_f is the tyre cornering stiffness.